LANGMUIR

pubs.acs.org/Langmuir Article

Adsorption of Hydrophilic Silica Nanoparticles at Oil−Water Interfaces with Reversible Emulsion Stabilization by Ion Partitioning

Robert K. Keane, Wei Hong, Wei He, Sam Teale, Robbie Bancroft, and Anthony D. Dinsmore*

Cite This: *Langmuir* 2022, 38, 2821−2831 Read Online

ACCESS | Metrics & More | Article Recommendations | Supporting Information

ABSTRACT: Adsorption of particles at oil−water interfaces is the basis of Pickering emulsions, which are common in nature and industry. For hydrophilic anionic particles, electrostatic repulsion and the absence of wetting inhibit spontaneous adsorption and limit the scope of materials that can be used in emulsion-based applications. Here, we explore how adding ions that selectively partition in the two fluid phases changes the interfacial electric potential and drives particle adsorption. We add oil-soluble tetrabutyl ammonium perchlorate (TBAP) to the nonpolar phase and Ludox silica nanoparticles or silica microparticles to the aqueous phase. We find a well-defined threshold TBAP concentration, above which emulsions are stable for months. This threshold increases with the particle concentration and with the oil's dielectric constant. Adding $NaClO_4$ salt to water increases the threshold and causes spontaneous particle desorption and droplet coalescence even without agitation. The results are explained by a model based on the Poisson−Boltzmann theory, which predicts that the perchlorate anions (ClO_4^-) migrate into the water phase and leave behind a net positive charge in the oil. Our results show how a large class of inorganic hydrophilic, anionic nanoparticles can be used to stabilize emulsions in a reversible and stimulus-responsive way, without surface modifications.

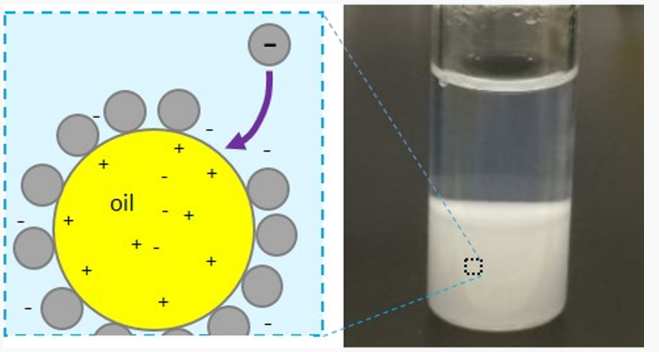

Downloaded via UNIV OF MASSACHUSETTS AMHERST on December 20, 2022 at 21:57:46 (UTC).
See https://pubs.acs.org/sharingguidelines for options on how to legitimately share published articles.

1. INTRODUCTION

Interfaces between immiscible fluids such as oil and water occur in many aspects of daily life including food and cosmetics. Under a wide range of conditions, particles suspended in either fluid strongly attract fluid interfaces and tend to bind or adsorb there.[1−3] This phenomenon provides a mechanism of stabilizing emulsions without the use of molecular surfactants. These particle-stabilized (also called "Pickering") emulsions are used in food and oil-recovery applications.[4−14] Particle-coated interfaces also create new opportunities to fabricate nanoparticle-based elastic capsules (built around droplets) or sheets (built on planar interfaces) that are soft and deformable and also endowed with the electronic, optical, or catalytic properties of the particles.[15−24] A prominent driving force for particle adsorption at the interface is interfacial tension, often described using the model of Koretsky, Kruglyakov,[2] and Pieranski.[3] At the continuum scale, the binding energy is related to the Young−Dupré equilibrium contact angle, where the two fluids and the solid surface meet. This model accounts successfully for the (often quite strong) binding of uncharged, partially hydrophobic particles at interfaces, where the particles are partially wetted.[4,25] As has been noted previously,[26] however, this model does not account for interactions between charged particles and the interface (which can spontaneously develop negative charge[27−38]) or the image charge induced in the dispersed fluid.[39−43] Because of the charge, forming Pickering emulsions from small, anionic, hydrophilic particles has proven to be challenging because the particles tend not to bind or to bind only weakly.[44−46] Solutions to this problem include adjusting the pH to reduce charge,[47,48] making their surface hydrophobic to partially wet the dispersed fluid,[6,46] reversing the particle surface charge,[49] or adding a costabilizer that causes the aggregation of the particles and enhances their binding at the interface.[44,50−52] In applications, these steps may cause undesired consequences such as the aggregation of particles in the bulk.

Adjusting the interfacial potential is a useful alternative way to control particle binding. For example, an electric potential can be applied across the interface using an electrochemical cell, which drives particles to adsorb or desorb.[24,53,54] Systems of this kind are often referred to as "interfaces between immiscible electrolyte solutions" or ITIES.[55] In systems where ions with only one sign of charge can transfer across the

Received: November 1, 2021
Revised: January 23, 2022
Published: February 21, 2022

ACS Publications © 2022 American Chemical Society

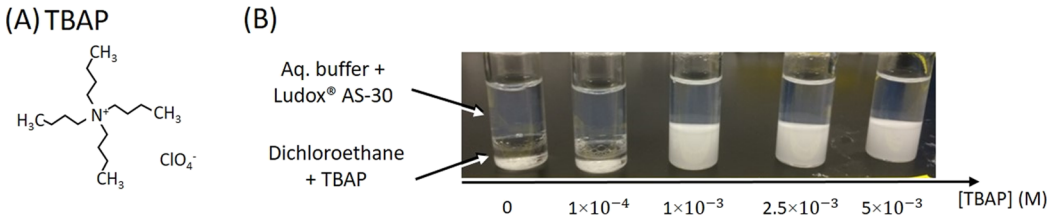

Figure 1. (A) Structure of TBAP, with its large hydrophobic cation and small anion. (B) Photographs of five samples, 1 h after shaking. Samples had 1 wt. % anionic silica nanoparticles in the aqueous phase and TBAP in the DCE phase with concentrations as shown below in the images. The two samples at the left separated into an aqueous phase floating on the oil (DCE + TBAP) phase. The three samples on the right retained oil droplets suspended in the aqueous phase. These emulsions remained stable for many weeks and showed no visible signs of coarsening.

interface, a potential drop (Galvani potential) can arise spontaneously—without an externally applied potential—and thus drive or prevent particle adsorption.[56−59] This effect is similar to the Donnan potential that arises in the presence of a membrane that is ion-selective; here, the different solubilities of the ions play the role analogous to membrane selectivity. The potential at the interface can be tuned via the total ion concentration.[55,59−61] There are several practical advantages of tuning the interface potential via the ion concentration: there is no need for electrodes, the stability of the particles in the bulk suspension is not compromised (as it can be, for example, with changing pH), and the ion concentration can be changed to tune emulsion stability dynamically and recover the dispersed phase in bulk. Leunissen and co-workers have investigated the ion-partitioning effect in a suspension of weakly charged particles in oil (cyclohexyl bromide and *cis*-decalin), in which the water side of the interface gained the net charge from the partitioning of anions from oil into the water phase.[56,57] (These ions were present in the oil phase as a residual from their manufacture.) More recent experiments showed conclusively that the charged, oil-dispersed particles provided emulsion stability even without breaching the water−oil interface,[58] which can be explained by electrostatic image attraction.[41,58] Experiments also showed that adding ions to the oil phase altered the charge on the colloidal particles so that they spontaneously desorbed from the interface.[58] Together, these studies showed that Pickering emulsions can be formed by electrostatic plus van der Waals forces—without the capillary forces in the model of Koretsky, Kruglyakov, and Pieranski.

The next step is to develop the use of ion partitioning with added ions, to explore its effect on emulsion stability, and to extend its application to water-dispersed hydrophilic particles. Recent work by Zheng and co-workers showed that the addition of tetraalkylammonium salts to water + octane + silica nanoparticles led to particle adsorption and Pickering emulsions above a threshold salt concentration.[49] Intriguingly, stable emulsions were found at salt concentrations low enough that the particles' zeta potential was unaffected,[49] suggesting to us the possibility that ion partitioning may have played an important role. Remaining questions include the role of the sign of the particles' charge, the effect of the oil used, and a comparison of emulsion stability to models that account for ion partitioning.

In this article, we report on experiments with hydrophilic silica nanoparticles, with silica microparticles, and with millimeter-scale borosilicate glass beads. We found that nonfunctionalized anionic nanoparticles could stabilize emulsions of dichloroethane, dichloromethane, or trichlorobenzene only when a selectively partitioning salt was dissolved in the oil phase. We chose tetrabutyl ammonium perchlorate (TBAP), which has a large hydrophobic cation[61−63] that remains in the oil and a small hydrophilic anion (Figure 1A) that can transfer to water. We varied the concentrations of TBAP in oil and of $NaClO_4$ in water and found a sharp threshold between unstable and stable emulsions. We mapped the behavior in terms of ion concentrations and particle concentrations for two oils of different dielectric constants. From optical images, we found that the microparticles adhered to the interface but apparently did not breach it. We also found that stable emulsions ruptured spontaneously (without shaking) when $NaClO_4$ salt was added to the aqueous phase, owing to an adjustment of the ion partitioning because of the added ClO_4^-. Finally, we found the reverse behavior with cationic silica nanoparticles: TBAP partitioning suppressed emulsion formation. To model our results, we account for the free energy of partitioning ions, then find the double-layer attraction between the interface and the charged nanoparticles. The model agrees reasonably well with our experimentally determined conditions, leading to stable emulsions and may explain the results of a prior study with octanol emulsions.[49] Together, our results show that stable emulsions can be formed using ions to control interfacial charge. We also demonstrate particle-stabilized emulsions that can spontaneously break up by the addition of salt water, leading to the potential for stimuli-responsive emulsions. These findings open the door to using water-dispersed, hydrophilic anionic particles (which are inexpensive and plentiful) as emulsion stabilizers, without chemical modifications of their surfaces.

2. MATERIAL AND METHODS

Most of these experiments were performed with anionic nanoparticles Ludox AS40 colloidal silica (Sigma-Aldrich, 7631-86-9), a 40 wt. % particle suspension. The diameter of the Ludox AS nanoparticles is approximately 22 nm,[64] and the zeta potential ranges from −30 to −18 mV at pH 5.7 when the NaCl concentration ranges from 4×10^{-5} to 10^{-2} M (a range of salinity that is similar to the conditions in our study).[65] To prepare samples with lower wt. %, we diluted the Ludox AS stock in pH 8 buffer containing NaOH, KCl, and boric acid (Fisher Scientific, S25208G). Cationic nanoparticles were Ludox CL colloidal silica (Sigma-Aldrich, 420,883), a 30 wt. % particle suspension. The diameter of the Ludox CL nanoparticles is approximately 12 nm (by TEM[66]), and the zeta potential is approximately 40 mV near neutral pH.[66] To obtain lower wt. %, we diluted the stock suspension with filtered, deionized water. In some experiments, we used 1.4 μm diameter "micropearl" silica spheres (Sekisui Chemical Co., Shiga, Japan, type SI-H014), received in the form of a powder and suspended in pH 8 buffer.

We used three different nonpolar solvents for the "oil" phase. (i) 1,2-Dichloroethane (DCE; Fisher Scientific, cat. no. E175−500; mass density = 1.25 g/cm^3 and dielectric constant ε = 10.4) (ii) Dichloromethane (DCM; Fisher Scientific, cat. no. 75-09-2; mass

https://doi.org/10.1021/acs.langmuir.1c02919
Langmuir 2022, 38, 2821−2831

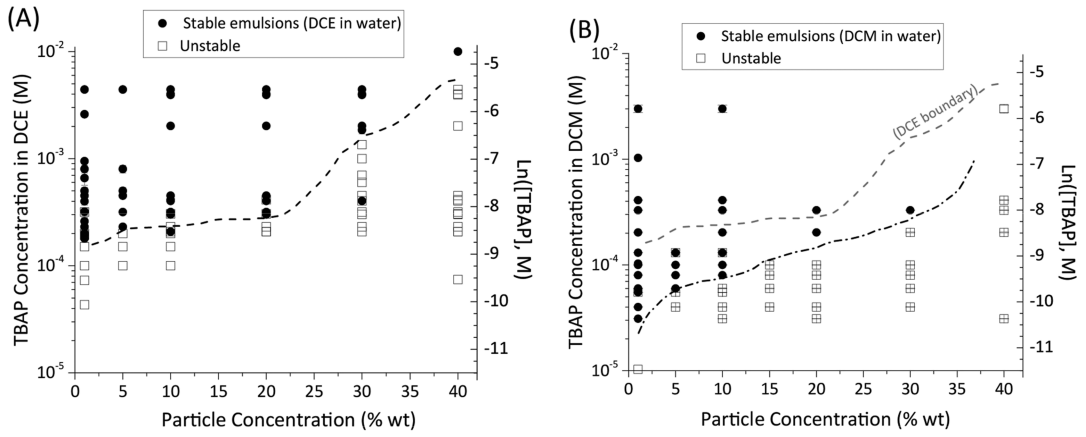

Figure 2. Diagrams showing the regions of stability of oil-in-water emulsions stabilized by anionic silica nanoparticles. The concentration of Ludox AS silica nanoparticles in the aqueous phase is on the horizontal axis. (A) DCE as the oil phase. The concentration of TBAP in the DCE phase is on the left vertical axis, and its logarithm is on the right axis. (B) DCM as the oil phase. In both cases (A, B), we found a distinct boundary between stable emulsions (higher [TBAP], lower particle concentration) and unstable emulsions. The dashed curves are a guide to the eye, separating the regions in which the great majority of samples were stable *vs* unstable. The stability threshold curve for DCE was reproduced on the DCM plot for comparison.

density = 1.33 g/cm^3 and ε = 8.9). (iii) 1,2,4-Trichlorobenzene (TCB; Sigma-Aldrich, cat. no. 296104, mass density = 1.45 g/cm^3 and ε = 2.4).

TBAP (GPS Chemicals, 1923-70-2) was dissolved in the oil phase prior to preparing emulsions. (Figure 1A shows the molecular structure.) TBAP concentrations (denoted as [TBAP]) and uncertainties were measured with a Mettler AE10 balance. TBAP readily dissolved in DCE and DCM at concentrations up to 0.1 M. In TCB, however, the TBAP solubility was below 0.01 M.

Samples were prepared in 15 × 45 mm glass vials precleaned with methanol. For our state diagram studies, 1 mL each of the aqueous and oil phases were added to each vial. Borosilicate glass pipets were used to transfer all oil phases. This 1:1 volume ratio was maintained to prevent a bias toward water-in-oil or oil-in-water emulsions. Vials were sealed and shaken vigorously using hand with a timeline described below. In some cases, after obtaining stable emulsions, we subsequently added an aqueous solution of $NaClO_4$ and either agitated the sample or allowed $NaClO_4$ to diffuse into the sample. The results of these experiments are described below.

3. RESULTS AND DISCUSSION

We prepared emulsions by mixing an aqueous suspension of anionic silica particles (Ludox AS) with an oil phase, either DCM, DCE, or TCB containing TBAP. In all cases, the emulsions were not stable if no TBAP was added or if the TBAP concentration was $<10^{-5}$ M. Instead, those samples were phase-separated within minutes, as shown in the example of Figure 1B, where the aqueous phase floats atop DCE. A striking result of our experiments is that with TBAP present above a threshold concentration, the emulsions were stable for several weeks or longer. Figure 1B shows examples of oil-in-water emulsions 1 h after shaking. The three samples with [TBAP] $\geq 10^{-3}$ M had clearly defined opaque regions, which consisted of DCE droplets that sedimented at the bottom of the aqueous phase. These droplets were clearly visible to the eye and via optical microscopy (Figure S1 of the online supplementary materials). In the absence of silica particles, emulsions were never stable even with TBAP up to 0.1 M. Likewise, stable emulsions of DCE were never found using 1 wt. % cationic Ludox CL for any [TBAP] between 0 and 0.1 M.

3.1. State Diagrams. Figure 2A shows the regime in which stable emulsions were obtained with anionic Ludox AS and TBAP + DCE. The vertical axis is [TBAP] (defined as moles per liter of the oil phase), and the horizontal axis is the concentration of silica nanoparticles, which is defined as the percentage weight in the aqueous phase. Each symbol represents one sample. There were 97 samples in total, some of which were at the same concentrations. In every case, there were equal volumes of the oil and aqueous phases. To obtain consistent results, samples were vigorously shaken by hand for 10−15 s, then shaken again every 15 min over a period of 1 h. After shaking, samples were left undisturbed on a countertop. We defined emulsions as "stable" (against coalescence) if there was no visible droplet coarsening or coalescence 1 h after we stopped shaking the samples. In practice, however, these samples were stable for many weeks, except for those very close to the stability boundary. As an example of the latter, a sample containing 2.03 × 10^{-4} M TBAP and 1 wt. % was stable 1 h after shaking (so it counts as stable in Figure 2A), but visibly separated into bulk phases after a few hours.

On the plot, the dashed curve, drawn by the eye, separates the regions of parameter space corresponding to stable vs unstable emulsions. One sample, at 30% Ludox and approximately 3 × 10^{-4} M TBAP, did not follow this trend (i.e., lay within the unstable region but appeared to be stable). This composition was repeated with a new preparation and found to be unstable. Both symbols are shown on the plot, but it seems likely to us that the first sample was made in error or was contaminated. In DCE samples containing 1 wt. % silica nanoparticles, the measured threshold concentration was (1.6 ± 0.2) × 10^{-4} M. When the particle concentration was 5 wt. %, the stability threshold increased to approximately (2.1 ± 0.2) × 10^{-4} M. The threshold value of [TBAP] was monotonically higher in samples with higher concentrations of nanoparticles, increasing modestly up to 20 wt. % and then increasing quite sharply at higher concentrations.

Figure 2B shows the stability diagram for DCM, which is slightly less polar than DCE. We prepared 56 separate samples, and their responses are shown in the plot. The overall trend is similar, but in DCM, the threshold [TBAP] was noticeably lower. For 5 wt. % nanoparticles, the threshold [TBAP] was approximately (6 ± 1) × 10^{-5} M, which is lower than the corresponding value in DCE by a factor of 3.5 ± 0.7. As was

https://doi.org/10.1021/acs.langmuir.1c02919
Langmuir 2022, 38, 2821−2831

found with DCE, there were three cases of outlying points, which were repeated and found to follow the trend of the other 53 samples. In Figure 2B, we show a sketched threshold between the stable and unstable emulsions (dash-dot curve). We superimposed the threshold curve obtained from the DCE data. Below, we show how that difference arose from the dielectric constants of DCE and DCM.

3.2. Emulsification of TCB with Anionic and Cationic Silica Nanoparticles. We repeated the emulsification test using TCB as oil in place of DCE. Using 1 wt. % Ludox AS silica as the aqueous phase, we found results qualitatively consistent with those of DCE and DCM: emulsions were not stable in the absence of TBAP, and they were stable for at least a month with 0.007 M TBAP (Figure S2). Using 1 wt. % cationic Ludox CL, we found the reverse: emulsions of just TCB were stable for more than a month, while emulsions with 0.007 M TBAP coalesced and phase-separated in a few minutes (Figure S2). In the absence of particles, emulsions were not stable. As will be discussed below, these results suggest that the TCB−water interface spontaneously developed a negative potential that attracted the CL nanoparticles and that TBA^+ partitioning reversed the sign of the charge at the interface.

3.3. Optical Images of Silica Particles and a Glass Sphere at the Interface. Evidence that Ludox AS silica nanoparticles bind at the DCE−water interface was provided by optical images. The nanoparticles are too small to see directly using an optical microscope, but we found indirect evidence of their adsorption by exposing DCE droplets to bright illumination in the microscope, so that heating led to DCE evaporation and droplet shrinkage. As the droplets shrank, they adopted wrinkled and nonspherical shapes, which we attribute to a jammed layer of particles. After further shrinkage, sheetlike structures were seen delaminating from the droplet surfaces, which indicate nanoparticles that adsorbed and then aggregated at the interface (Supporting Information Figure S1).

We repeated the imaging experiments using 1.4 μm diameter silica spheres instead of the silica nanoparticles. In the absence of TBAP, particles did not bind at the interface. With 1 M TBAP, however, we found a close-packed monolayer of microparticles bound at the surface of a DCE droplet, as shown in Figure 3. The spheres spontaneously formed well-ordered arrays because of their narrow size distribution (approx. 1% size variation). We also found that the particle binding at the interface was reversible: when the droplets were heated by the microscope illumination, the droplets gradually shrank and then disappeared, and the silica spheres freely diffused away without aggregation.

We used confocal microscopy to distinguish whether the 1.4 μm diameter silica microparticles were bound to the interface or, on the other hand, partially inserted into (breached) the interface. We added a green, fluorescent fluorescein dye to the aqueous phase and fluorescent Nile red dye to the DCE phase, which also contained 0.01 M TBAP. Figure S3 of the online supplementary section indicates that particles lay next to the interface. They either did not breach the interface at all, or only barely did so with a low contact angle.

Finally, we used millimeter-scale borosilicate glass spheres at water−DCE interfaces. With these much larger particles, we could obtain precise measurements of the contact angle. We note, however, that the surface properties of borosilicate glass are not the same as those of silica nanoparticles, so the interfacial tensions differ. Indeed, we found that the glass sphere was partially wet by DCE (i.e., it breached the interface), which is in contrast to our result for the 1.4 μm silica. To measure the contact angle, we attached a glass sphere to a small glass rod and pulled the sphere upward through the interface (water floating on DCE; see the Supporting Information). On a few occasions during the process, we halted the motion and allowed the flow to stop. This protocol gave us the receding angle. For a pure water−DCE interface (no TBAP), we found a receding contact angle of $\theta_R = 96°$. Using the same glass sphere with 0.05 M TBAP in DCE, we found $\theta_R = 130°$ (Figure S4). These results indicate a reduction in the interfacial tension between the particle and the oil phase and a greater binding energy. As in the previous cases, partitioning of TBAP anions is the key; however, here, the particle is partially wet by the oil, so the interactions differ. We return to this point below.

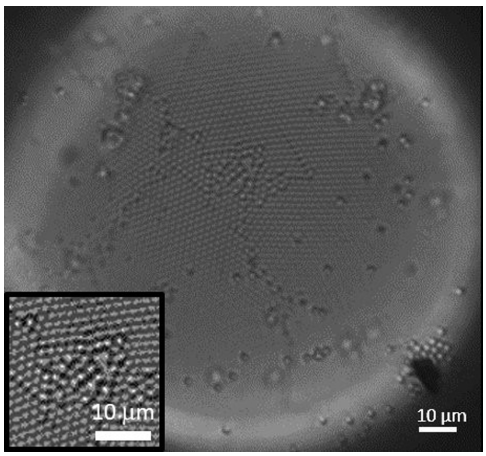

Figure 3. Optical microscope image of a DCE droplet with 1 M TBAP, coated using a layer of 1.4 μm diameter silica spheres. The inset shows an expanded section of the center of the image in the main panel.

3.4. Competition with Water-Based Ions and Reversibility. To see whether other ions in the aqueous phase can compete with the favorable effect of TBAP, we added sodium perchlorate ($NaClO_4$) to the aqueous phase. We chose $NaClO_4$ because it has the same anion and replaces the bulky hydrophobic cation with the small hydrophilic Na^+. We prepared samples with 1 wt. % silica nanoparticles and varying [TBAP] and [$NaClO_4$], mixed them, and assessed emulsion stability as described above. Figure 4 shows the results for DCE. We found that added $NaClO_4$ prevented stable emulsions with a monotonic trend shown in Figure 4B. The dashed curve shows the boundary between stable and unstable emulsions. At low concentrations, the boundary lies near the line [$NaClO_4$] = [TBAP]. Once the aqueous salt concentration approached 0.1 M, a much higher [TBAP] was necessary to stabilize the emulsions.

We also found that adding $NaClO_4$ to a stable emulsion can break the emulsion, leading to bulk-phase separation. When we added $NaClO_4$ to the aqueous phase and shook it by hand, emulsions separated within approximately a minute. An example is highlighted by the black box in Figure 4A, where [$NaClO_4$] was increased from 0.005 to 0.05 M. Remarkably, the emulsions destabilized spontaneously even without convection, when $NaClO_4$ was gently added to the aqueous phase without shaking. In the Supporting Information, we

https://doi.org/10.1021/acs.langmuir.1c02919
Langmuir 2022, 38, 2821−2831

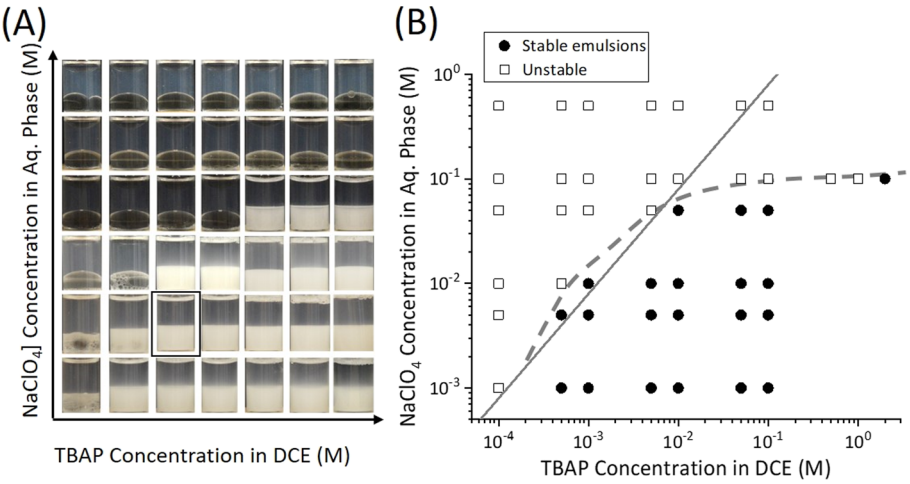

Figure 4. (A) Array of images with DCE + TBAP mixed with an aqueous phase containing varying amounts of $NaClO_4$. The Ludox AS silica nanoparticle concentration was fixed at 1 wt. %. Samples with higher [TBAP] and lower [$NaClO_4$] tended to form stable emulsions, which are visible as the white sediment. The sample with the box around it spontaneously separated when [$NaClO_4$] was increased from 0.005 to 0.05 M. (B) Same results in the form of a plot. The dashed curve is a guide to the eye, separating the regions in which samples were stable vs unstable. The gray solid line shows the prediction of the theory described in the text.

show images of a sample with 4×10^{-4} M TBAP in DCE with and 1 wt. % silica nanoparticles with no added $NaClO_4$. This sample formed a stable emulsion. We then added 1 mL of 0.02 M $NaClO_4$ to the top of the sample gently, without mixing. We let the solution sit undisturbed and found that the droplets coalesced and formed two separate fluid phases over a period of 20 h (Supporting Information Figure S5). This slow rate of coalescence might be limited by the slow rate of diffusion or by the slow rate of escape of particles from the interfaces. In either case, the reversibility indicates that the particles bound weakly enough that they could escape by thermal fluctuations. The mechanism by which $NaClO_4$ reduces the binding will be discussed below.

3.5. Discussion of Mechanisms that Control Particle Binding. With anionic nanoparticles and TBAP concentrations between 0 and 10^{-5} M, we found no stable emulsions, which indicates that nanoparticles adsorbed at low coverage or not at all. We found by direct observation that the 1.4 μm silica particles did not adsorb unless TBAP was present. With higher [TBAP], nanoparticles adsorbed, and stable emulsions were readily formed. The confocal images of 1.4 μm diameter silica spheres indicated that particles adhere to but do not penetrate into the oil phase (or only just barely did so). All of our emulsions were oil droplets in water, consistent with the common trend (Bancroft's rule) in which the continuous phase contains the stabilizing agents.

In the absence of TBAP, the lack of anionic silica particle adsorption is attributed to the lack of wetting: the particles are hydrophilic so that capillary forces disfavor breaching the interface. There may also be a negative electric potential at the fluid interface and hence double-layer repulsion of the negatively charged particles (Figure 5A). Examples of a negative potential at the fluid interface are found in previous electrokinetic measurements,[27−32,67,68] theory, and simulation,[33−38] which report potentials of approximately −30 mV relative to the aqueous bulk, depending on the pH and salinity. Examples include nonpolar solvents with dielectric constants ranging from near 2 (alkanes, xylene, and benzene[27−32,67,68]) to 25 (nitrobenzene[29]). The negative electric potential has often been attributed to the adsorption of OH^-[28−30,32] or

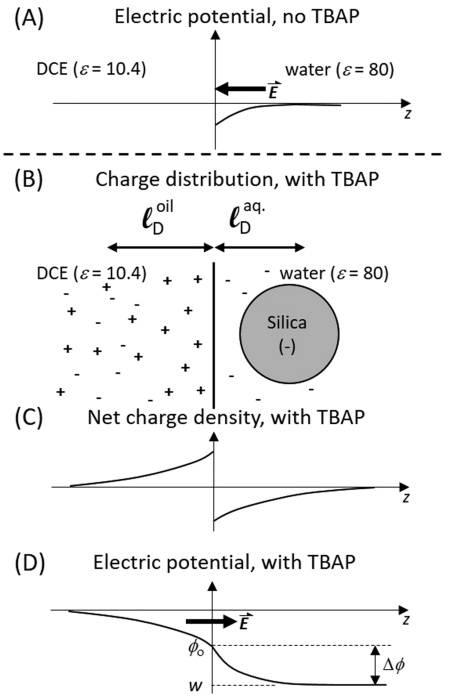

Figure 5. (A) Schematic of the electric potential in the aqueous phase with no added TBAP, leading to an electric field ($\boldsymbol{E}$) that repels negative particles in water. (B–D) Partitioning of the ClO_4^- anions from the DCE phase into the aqueous phase, while the hydrophobic TBA^+ ions remain in DCE. The charge separation gives rise to a charge density shift, as illustrated in (C). The result is an electric field to the right and an electric potential curve illustrated in (D).

other anions[69] at the interface, although there may be competing conclusions from nonlinear optical probes.[70] Theoretically,[37] ab initio computer simulations[34] and molecular dynamics simulations[33,36] also support the idea that OH^- ions accumulate at the interface. In addition to the double-layer repulsion, there should be an "image" repulsion arising from the polarization of the lower-dielectric constant oil phase.[39,40,42,43]

https://doi.org/10.1021/acs.langmuir.1c02919
Langmuir 2022, 38, 2821−2831

We found that cationic Ludox CL particles stabilized TCB emulsions ([TBAP] = 0), indicating that this interface developed a spontaneous negative potential. With DCE and DCM, we never found stable emulsions with cationic particles, which indicates that these liquids did not form a negative potential or that it was too small to overcome image repulsion of the particles.

By contrast, adding TBAP to the oil phase led to the adsorption of anionic silica particles at the oil−water interface with sufficient coverage to prevent coalescence of the droplets. Conversely, TBAP led to the repulsion of cationic particles and no emulsion formation. One might wonder whether anionic particle adsorption is driven by the condensation of the TBA+ ions onto the particle surface, thereby making the particles neutral and sufficiently hydrophobic to breach the interface (as found in other systems[71−73]). Prior studies of the adsorption of tetraalkyl ammonium ions into colloidal silica surfaces provide insight into this point. For a five-carbon alkyl chain (which is more surface-active than the 4-carbon TBAP), the zeta potential of silica in aqueous suspension decreased from −65 mV when the ion concentration exceeded roughly 10^{-6} M, but the reported change in zeta potential was low in magnitude.[74] At 10^{-3} M in water, the zeta potential was still near −50 mV.[74,75] Further insight comes from a recent study showing Ludox-stabilized octanol emulsions in water when the concentration of tetrabutyl ammonium nitrate exceeded a threshold on the order of 10^{-5} M, which was well below the concentration at which the particles' zeta potential was increased by the salt.[49] In our experiments, the concentrations of TBA+ ion in the aqueous phase are estimated on the order of 10^{-6} M near the threshold of emulsion stability, hence the effects of adsorption on zeta potential should be very small. As further evidence, we found that adding TBAP caused cationic silica to desorb from the interface (opposite to the behavior of anionic particles); in this case, there is no electrostatic drive for TBA+ to bind on the particle; hence, desorption of the particles must have a different mechanism.

One might also wonder whether TBAP itself partitions to the interface, owing to the presence of hydrophobic and hydrophilic moieties. Prior measurements of the air−water interfacial tension in the presence of TBA salts show a very small effect on the air−water interfacial tension (<1 N/m) at concentrations below approximately 0.001 M.[76] In our work, the threshold concentrations in oil are roughly 10× lower than this, and the concentrations in the water phase are roughly 10^6× lower (see below). Therefore, at the aqueous-phase concentrations that are relevant for our experiments, the interfacial affinity of the TBA+ ions should be exceedingly small, in terms of change in interfacial tension. (Indeed, no emulsions formed with TBA and no particles.) Based on these literature reports, therefore, we conclude that TBA+ adsorption at the interface or on the particle surfaces is not the driving mechanism.

Instead, our findings are explained by the partitioning of the perchlorate anions into the aqueous phase, where their electric potential energy is lower and the entropy is higher. The TBA^+ ions are retained in the oil phase owing to their hydrophobic alkyl chains. This partitioning leads to a net positive charge in the oil that attracts nearby anionic particles and repels cationic particles. Figure 5 illustrates this mechanism, which is described in the next section.

3.6. Model Based on Poisson−Boltzmann Theory. Here, we describe a model to account for ion partitioning and anionic particle adsorption. Our model follows approaches taken earlier[77,78] and, like them, we ignore the intermolecular and interparticle correlations and specific-ion effects that have been discussed elsewhere.[59,62,79] To quantify the extent of charge partitioning, we assume that the TBA^+ ions are trapped in the oil (which will be justified below) and consider only the concentration profile of the anions (ClO_4^-, in the experiment). We follow a standard Poisson−Boltzmann approach, in which the ions are treated as an ideal gas and their electrostatic interactions are described by an electric potential, $\phi(z)$, that depends on their spatial distribution. The z-axis is defined to lie perpendicular to the interface, the oil phase lies at $z < 0$, and the aqueous phase resides at $z > 0$ (Figure 5A). Because the ClO_4^- ions are the mobile species, their equilibrium distribution is determined by a uniform chemical potential. In the oil phase, the chemical potential $\mu(z)$ of the ClO_4^- ions is as follows:

$$\mu(z) = k_B T \ln(c_o(z)\Lambda^3) + (-e)\phi(z) + \epsilon_{B,o} + \mu_{solvation} \quad (1)$$

where $c_o(z)$ is the concentration of anions in the oil phase, Λ is the thermal wavelength, k_BT is Boltzmann's constant times the temperature (in Kelvins), and e is the elementary charge (a positive number). The parameter $\epsilon_{B,o}$ is the Born free energy for embedding a small, spherical charge in a low-dielectric-constant medium. This term plays the key role in driving the ions into the aqueous phase as described previously.[80] Finally, $\mu_{solvation}$ is the contribution from rearranging the solvent (oil) molecules around the ion. The bulk concentration of anions in the oil is c_o^∞, which is the same as that of [TBAP] because a negligible fraction of anions in the oil transfer to water (see the Supporting Information).

In the water phase, we account for the anions that were previously added to the aqueous phase at concentration c_s; this parameter corresponds to the vertical axis of Figure 4B. The chemical potential of the ClO_4^- ions in the aqueous phase is as follows:

$$\mu(z) = k_B T \ln((c_w(z) + c_s)\Lambda^3) + (-e)\phi(z) + \epsilon_{B,w} \quad (2)$$

where $c_w(z)$ is the concentration of partitioning anions in the aqueous phase, and $\epsilon_{B,w}$ is the Born energy for a charged spherical ion in water.

Within these same approximations, the electric potentials obey the Poisson−Boltzmann theory. Further assuming that the potential is small everywhere ($e\phi/k_BT \ll 1$), we use the Debye−Hückel approximation and obtain the following equations:

$$\phi(z) = \phi_0 e^{z/l_o}, \qquad z < 0$$
$$\phi(z) = (\phi_0 - w)e^{-z/l_w} + w, \; z \geq 0 \quad (3)$$

where ϕ_0 is the electric potential at the interface, and w is the potential far away in the aqueous phase. (Below, we note that $e\phi/k_BT$ is not always $\ll 1$ near the interface, which may lead to quantitative errors in our estimate of the threshold concentration.) We have made sure that the electric displacement field (commonly called $\boldsymbol{D}$) is continuous across the interface, which corresponds to assuming no space charge bound at the interface (which is distinct from the ion clouds *near* the interface). The parameters l_o and l_w are the Debye screening lengths in the oil and aqueous phases, respectively.

https://doi.org/10.1021/acs.langmuir.1c02919
Langmuir 2022, 38, 2821−2831

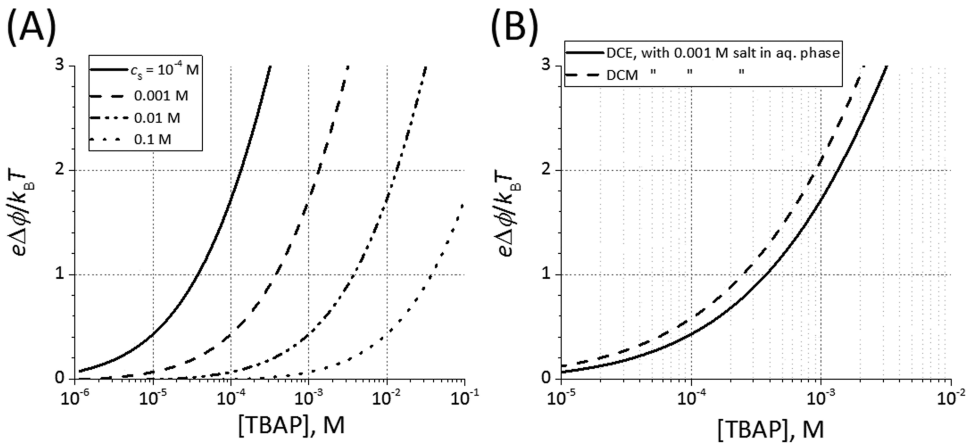

Figure 6. Plots of $e\Delta\phi/kT$ from the model, eq 5. (A) Predictions for DCE for various values of aqueous-phase salt concentration, c_s. (B) Predicted results for DCE and DCM and c_s = 0.001 M.

$$l_\alpha^2 = \varepsilon_0\varepsilon_\alpha k_B T/(2c_\alpha e^2) \quad (4)$$

where α refers to oil or aqueous, ε_α is the dielectric constant of the α phase, and ε_0 is the vacuum permittivity. These potentials are qualitatively sketched in Figure 5D.

To find the electric potential energy of a particle adsorbing at the interface from the aqueous bulk, the key is to determine the value of $\phi_0 - w$, which we call $\Delta\phi$. This quantity can be found by assuming that the total number of ions is conserved, that Gauss' law is satisfied, and that $c_w(z = \infty) = 0$. (Recall that c_w refers only to the partitioning anions coming from TBAP.) The result is as follows:

$$\frac{e\Delta\phi}{k_BT} = \left[\ln\left(\frac{c_o^\infty}{c_s}\right) + (\epsilon_{B,o} + \mu_{solvation} - \epsilon_{B,w})/(k_BT)\right] \left[\frac{1}{\left(1 + \sqrt{\frac{c_s\varepsilon_w}{c_o^\infty\varepsilon_{oil}}}\right)}\right] \quad (5)$$

The final factor on the right-hand side accounts for the Debye lengths of the oil and water phases, which depend on both ion concentrations and dielectric constants. This factor has a noticeable effect on the results and should not be neglected. The terms $\epsilon_{B,o} + \mu_{solvation} - \epsilon_{B,w}$ were found from electrochemical measurements tabulated by École Polytechnique Fédérale de Lausanne (EPFL) (which were formerly available online[81]). For ClO_4^- ions transferring from DCE to water, the tabulated value is approximately $\epsilon_{B,o} + \mu_{solvation} - \epsilon_{B,w} = 6.5 \pm 0.4\ k_BT$. We estimated the uncertainty from the spread of tabulated values; see the Supporting Information.

Figure 6A, B shows plots of the predicted $e\Delta\phi/k_BT$ as a function of c_o^∞, which is equivalent to [TBAP]. One should expect strong electrostatic attraction between the particles and the interface when $e\Delta\phi/k_BT$ is on the order of 1. We found the closest agreement with the data with a threshold value of 1/2 (i.e., $\Delta\phi \approx -12.5$ mV). When $c_s = 10^{-2}$ M, the predicted threshold [TBAP] in DCE is about 12×10^{-4} M, which is in reasonable agreement with the measured value of about $(7 \pm 2) \times 10^{-4}$ M (Figure 4). Larger values for the threshold $e\Delta\phi/k_BT$ shifts the trend toward larger threshold [TBAP] (e.g., to 4×10^{-3} M if $e\Delta\phi/k_BT = 1$).

A more comprehensive comparison of our model to the results is shown by the straight line in Figure 4B, which shows the predicted boundary between stable and unstable emulsions. The threshold value of $e\Delta\phi/k_BT = 1/2$ gave a reasonable agreement with the data at salt concentrations $c_s <$ 0.1 M. For nonpolar solvents that yield a spontaneous negative interfacial potential, a larger threshold value of $e\Delta\phi/k_BT$ should be expected.

For salt concentrations c_s near 0.1 M or greater, the model overstates the region of emulsion stability (Figure 4). In this limit, our approximations break down because of the correlation among the ions in bulk or near the interface, where the ion concentration is high. The extent of ion correlations can be estimated from the coupling constant Γ, defined as $\Gamma = l_B/d$, where l_B is the Bjerrum length $(=e^2/(4\pi\varepsilon\varepsilon_0 k_BT))$, and d is the mean distance between ions.[82] Using our model, we estimated Γ in the bulk and interface regions on both the water and oil sides. (See the Supporting Information for details.) For $c_s = 10^{-3}$ M and [TBAP] $= 2 \times 10^{-4}$ M in DCE (near threshold), we estimate $\Gamma = 0.07$ and 0.87 at the interface on the water and oil sides, respectively. The coupling constants are lower in the bulk. In this range, the Poisson–Boltzmann theory should apply with a reasonable accuracy. For $c_s = 0.1$ M and [TBAP] $= 3.3 \times 10^{-2}$ M, however (again near threshold), the estimated Γ increased to 0.32 and 3.8 on the water and oil sides, respectively. In this regime, we should not expect the Poisson–Boltzmann theory to be accurate owing to strong ion-ion correlations. Hence, our main conclusion is that this model captures the essential physics and allows us to make reasonable order-of-magnitude estimates for aqueous-phase salt concentrations $c_S <$ 0.1 M.

Because of the Born energy that drives the smaller anions into the aqueous phase, our model predicts that the ClO_4^- partitioning is stronger for oil with lower ε. We are not aware of the reported measurements of the free energy of ClO_4^- partitioning in DCM, but we can make an estimate from the tabulated DCE values. First, we assume that $\mu_{solvation}$ is the same, and then, we use the known Born energy to account for the different dielectric constants of DCE and DCM. For this purpose, we used the estimated ionic radius of ClO_4^- as 2.41 Å.[83] (See the Supporting Information for details). The result is $\epsilon_{B,o} + \mu_{solvation} - \epsilon_{B,w} = 8.4\ k_BT$ for DCM. This approach predicts that the threshold TBAP for DCM should be about 1.5× smaller than that for DCE. Hence, DCM should show a

https://doi.org/10.1021/acs.langmuir.1c02919
Langmuir 2022, 38, 2821−2831

stronger partitioning effect than DCE. The data of Figure 4 show that the threshold [TBAP] was indeed smaller for DCM by a factor of 3 or more, which is qualitatively consistent with the model. The difference between them might arise from the fact that at threshold, $e\Delta\phi/k_BT$ is not $\ll$1. Additionally, it may be that $\mu_{solvation}$ is greater for DCM than for DCE, or image-charge repulsion, which should be stronger for DCM than for DCE, led to an increased [TBAP] that is not accounted for in our model. (As suggested earlier, however, image-charge effects should not predominate for these small particle sizes.[40]) In general, our model leads us to expect that the ion-partitioning effect should be stronger in less polar solvents such as alkanes—provided that TBAP is soluble at the threshold concentration. For low-dielectric constant solvents such as alkanes, the latter constraint may be prohibitive.

We have assumed that TBA^+ ions do not transfer to the aqueous phase. This assumption is supported by the measured transfer free energy for TBA^+,[81] which is 13 k_BT different from ClO_4^- (strongly disfavoring TBA^+ transfer to water). This implies that the ratio of concentrations of TBA^+ to ClO_4^- in water would be about e^{-13} or about 10^{-6}. We have also neglected the possibility that Ludox particles bound at the interface might alter the potential nearby, as discussed previously,[59] or that the particle charge changes by ion adsorption or charge regulation[26] (as in oil-dispersed particles of prior work[57,58]). These would be useful topics of future study if combined with quantitative measurements of particle surface coverage.

The time needed for the ClO_4^- ions to repartition and for $\Delta\phi$ to reach equilibrium is not readily estimated, as it depends on the details of the ion distribution at the interface itself. From the experiments, however, it is clear that the timescale is at least a few minutes because we had to continue shaking the samples for at least this long in order to obtain repeatable results. This remains an interesting topic for future study. If, for example, the timescale for the buildup of the interfacial charge can be made short enough, interfacial charging might be an effective way to drive particles to interfaces and rapidly stabilize the nonequilibrium structure such as bijels.[21,22]

3.7. Adsorption vs Breaching. Having established a double-layer attraction between the interface and the silica particles when TBAP is present, we now return to the question of whether one should expect the particles to penetrate partway into the oil phase. Neglecting electrostatic effects and assuming equilibrium, particles should breach the interface when there is a finite three-phase contact angle, that is, when $\gamma_{pw} - \gamma_{ow} < \gamma_{po} < \gamma_{pw} + \gamma_{ow}$ (where γ is the interfacial tension and subscripts o, w, p refer to oil, water, and particle, respectively).[2,3] Because the particles are hydrophilic, γ_{pw} is very likely smaller than γ_{ow}. Therefore, the left-most side of this equality is likely negative, and the first condition should be satisfied. For charged silica particles, however, the value of γ_{po} may be quite high because of the high free energy cost of transferring the dissociated charges into oil. The rationale is the same Born-energy argument described above. Thus, the second inequality condition is likely violated (i.e., we expect $\gamma_{po} \geq \gamma_{pw} + \gamma_{ow}$). Because of these surface charges, it is quite reasonable that the silica particles would be electrostatically attracted to the interface and yet not breach it. This argument is consistent with our results, although we were unable to rule out the possibility that microspheres bind with a low contact angle. This argument also explains our finding that silica particles could spontaneously desorb when the salinity was increased. By contrast, charged latex particles often irreversibly breach the interface, which we attribute to hydrophobic patches on their surface that lower γ_{po} and satisfy both inequalities.

We found that a millimeter-scale borosilicate glass sphere breached the interface and formed a finite receding contact angle at the pure DCE−water interface. The angle, measured through the aqueous phase, increased from 96° to 130° with added TBAP. (The surface properties of borosilicate glass are not the same as those of silica nanoparticles, so this result does not contradict the silica results.) Using the Pieranski/Koretsky model, we can estimate the binding energy for a particle approaching from the aqueous phase: $E_B = \pi R^2 \gamma_{ow}(1 - \cos\theta)^2$, where θ is the contact angle measured through the aqueous phase. From the measured θ, we find that E_B increased by a factor of approximately 2.2 when [TBAP] increased from 0 to 0.05 M. Here, unlike the nanoparticle case, the glass surface was partially wetted by the oil, so there was no double-layer attraction between the particle and the interface. Instead, we propose that the high concentration of TBA^+ cations in the oil served as counterions for the surface-bound silanol groups, leading to an entropic gain from the release of the water-based counterions. This effectively reduces γ_{po} and $\cos\theta$ and thereby increases E_B.

4. CONCLUSIONS

We found that the anionic charge and hydrophilicity of silica particles prevented the adsorption of anionic Ludox silica particles, but that adding TBAP to the bulk oil drove adsorption. As a result, nonfunctionalized hydrophilic, anionic silica particles stabilized Pickering emulsions when the TBAP concentration in the oil phase exceeded a well-defined threshold concentration. The measured values of the threshold [TBAP] were $(2.1 \pm 0.2) \times 10^{-4}$ M for DCE and $(0.6 \pm 0.1) \times 10^{-4}$ M for DCM with 5 wt. % anionic Ludox AS in water. We attribute this stabilization to the trapping of TBA^+ cations in the oil phase and partitioning of the ClO_4^- ions into the water phase, where the electrostatic energy is lower and the entropy is higher. This partitioning leaves a net positive charge from TBA^+ inside the oil near the interface, and it increases the electrostatic potential on the aqueous side of the interface relative to the aqueous bulk. Correspondingly, we found that cationic Ludox CL had a different trend: we found adsorption and stable emulsions with pure-TCB droplets (attributed to spontaneous negative interfacial potential) and no emulsions with added TBAP.

We explained our results using the Poisson−Boltzmann theory combined with previous measurements of the transfer free energy of the TBA^+ and ClO_4^- ions. The model successfully explains our results, agrees with the measured threshold [TBAP] values within a factor of approximately 2, and accounts for the different characteristics of DCE and DCM. As long as TBAP or a similar electrolyte dissolves in the oil phase, the same partitioning effects should be found for a wide range of oils. A relevant comparison is the octanol-in-water example reported earlier, where $TBANO_3$ added to the aqueous phase at 5×10^{-5} M led to silica-stabilized emulsions, even though the silica zeta potential was apparently unaffected by $TBANO_3$. Octanol has a dielectric constant similar to DCE, so it may be that the TBA+ cations partitioned into the oil phase and created an interfacial charge, as described here. Our model also accounts for the competitive—and reversible—effect of salt added to the aqueous phase at concentrations

https://doi.org/10.1021/acs.langmuir.1c02919
Langmuir 2022, 38, 2821−2831

below 0.1 M. At higher concentrations, however, the model greatly overestimates the emulsion-stabilizing effect owing to correlations among the ions.

While it appears to be generally the case that hydrophilic silica particles cannot emulsify oils near neutral pH and without surface modifications,[44−46] there is at least one exception: the polar oil diisopropyl adipate.[51] Even in that case, lowering the pH (and hence the particle charge) improved emulsion stability, presumably by lowering the repulsion of the charged interface. As far as we are aware, it remains unclear how to predict which oils spontaneously lead to a high interfacial potential when dispersed in water. We anticipate, although, that the addition of partitioning ions such as TBAP will always favor anionic particle binding, and the addition of competing salts such as $NaClO_4$ will always tend to suppress it.

Our results provide two important developments for applications. First, tuning the electrostatic interfacial potential allows Pickering emulsions to be formed with as-made silica particles without modifying their surfaces to make them partially hydrophobic. This approach opens the door to use a large class of inorganic colloids (which are often hydrophilic and anionic) without surface modifications. Second, particle adsorption is reversible: adding salt to the aqueous phase causes the particles to desorb spontaneously, the emulsion droplets coalesce, and the oil and aqueous phases separate. This means that emulsions can be stable even if particles do not breach the interface, and the binding is reversible, as noted recently[41,58] and in contrast to earlier reports.[51] This also demonstrates that these emulsions are sensors of salinity, and emulsion-based materials might be made to coalesce and trigger chemical reactions in response to exposure to sea water. More generally, this study provides new insight into ion-driven electrostatic interactions that govern particle binding at fluid interfaces.

■ ASSOCIATED CONTENT

Supporting Information

The Supporting Information is available free of charge at https://pubs.acs.org/doi/10.1021/acs.langmuir.1c02919.

Images of anionic silica nanoparticles on DCE + TBAP droplets; emulsions of TCB and TBAP using anionic or cationic silica nanoparticles; confocal fluorescence images of 1.4-μm silica spheres at the water/DCE interface; measurements of receding contact angles of mm-sized borosilicate glass sphere; spontaneous coalescence in response to salt added to the aqueous phase; and details of the model based on the Poisson−Boltzmann theory (PDF)

■ AUTHOR INFORMATION

Corresponding Author

Anthony D. Dinsmore − *Department of Physics, University of Massachusetts, Amherst, Massachusetts 01003, United States;* orcid.org/0000-0002-0677-765X; Email: dinsmore@umass.edu

Authors

Robert K. Keane − *Department of Physics, University of Massachusetts, Amherst, Massachusetts 01003, United States*

Wei Hong − *Department of Physics, University of Massachusetts, Amherst, Massachusetts 01003, United States*

Wei He − *Department of Physics, University of Massachusetts, Amherst, Massachusetts 01003, United States*

Sam Teale − *Department of Physics, University of Massachusetts, Amherst, Massachusetts 01003, United States*

Robbie Bancroft − *Department of Physics, University of Massachusetts, Amherst, Massachusetts 01003, United States*

Complete contact information is available at: https://pubs.acs.org/10.1021/acs.langmuir.1c02919

Notes

The authors declare no competing financial interest.

■ ACKNOWLEDGMENTS

We thank the National Science Foundation for funding through CBET-1803797 and the Army Research Office for funding through the MURI program, grant W911NF-15-1-0568. Wei Hong also thanks the UMass Materials Research Science and Engineering Center (MRSEC) on Polymers, DMR-0820506, and the Xerox University Affairs Committee for their support.

■ ABBREVIATIONS

DCE, 1,2-dichloroethane; DCM, dichloromethane; TCB, trichlorobenzene; TBAP, tetrabutyl ammonium perchlorate

■ REFERENCES

(1) Pickering, S. U. Emulsions. *J. Chem. Soc.* **1907**, *91*, 2001−2021.

(2) Koretsky, A. F.; Kruglyakov, P. M. I. Emulsifying Effects of Solid Particles and the Energetics of Putting them at the Water-Oil Interface. *Izv. Sib. Otd. Akad. Nauk. SSSR Ser. Khim. Nauk.* **1971**, *2*, 139−141.

(3) Pieranski, P. Two-Dimensional Interfacial Colloidal Crystals. *Phys. Rev. Lett.* **1980**, *45*, 569−572.

(4) Binks, B. P. Particles as surfactants - similarities and differences. *Curr. Opin. Colloid Interface Sci.* **2002**, *7*, 21−41.

(5) Aveyard, R.; Binks, B. P.; Clint, J. H. Emulsions stabilised solely by colloidal particles. *Adv. Colloid Interface Sci.* **2003**, *100*, 503−546.

(6) Binks, B. P.; Murakami, R. Phase inversion of particle-stabilized materials from foams to dry water. *Nat. Mater.* **2006**, *5*, 865.

(7) Paunov, V. N.; et al. Emulsions stabilised by food colloid particles: Role of particle adsorption and wettability at the liquid interface. *J. Colloid Interface Sci.* **2007**, *312*, 381−389.

(8) Zhang, H. P.; et al. Investigation of OMA formation and the effect of minerals. *Mar. Pollut. Bull.* **2010**, *60*, 1433.

(9) Saha, A.; Nikova, A.; Venkataraman, P.; John, V. T.; Bose, A. Oil Emulsification Using Surface-Tunable Carbon Black Particles. *ACS Appl. Mater. Interfaces* **2013**, *5*, 3094−3100.

(10) Garbin, V. Colloidal particles: Surfactants with a difference. *Phys. Today* **2013**, *66*, 68−69.

(11) Sun, J.; Zheng, X. L. A review of oil-suspended particulate matter aggregation-a natural process of cleansing spilled oil in the aquatic environment. *J. Environ. Monit.* **2009**, *11*, 1801−1809.

(12) Abkarian, M.; Protiere, S.; Aristoff, J. M.; Stone, H. A. Gravity-induced encapsulation of liquids by destabilization of granular rafts. *Nat. Commun.* **2013**, *4*, 1895.

(13) Berton-Carabin, C. C.; Schroen, K. Pickering Emulsions for Food Applications: Background, Trends, and Challenges. *Annu. Rev. Food Sci. Technol.* **2015**, *6*, 263−297.

(14) Ortiz, D. G.; Pochat-Bohatier, C.; Cambedouzou, J.; Bechelany, M.; Miele, P. Current Trends in Pickering Emulsions: Particle Morphology and Applications. *Engineering* **2020**, *6*, 468−482.

(15) Velev, O. D.; Furusawa, K.; Nagayama, K. Assembly of Latex Particles by Using Emulsion Droplets as Templates. 1. Microstructured Hollow Spheres. *Langmuir* **1996**, *12*, 2374.

(16) Dinsmore, A. D.; et al. Colloidosomes: Self-Assembled, Selectively-Permeable Capsules Composed of Colloidal Particles. *Science* **2002**, *298*, 1006.
(17) Lin, Y.; et al. Ultrathin Crosslinked Nanoparticle Membranes. *J. Am. Chem. Soc.* **2003**, *125*, 12690.
(18) Lin, Y.; Skaff, H.; Emrick, T. S.; Dinsmore, A. D.; Russell, T. P. Nanoparticle Assembly and Transport at Liquid-Liquid Interfaces. *Science* **2003**, *299*, 226.
(19) Crossley, S.; Faria, J.; Shen, M.; Resasco, D. E. Solid Nanoparticles that Catalyze Biofuel Upgrade Reactions at the Water/Oil Interface. *Science* **2010**, *327*, 68.
(20) Duncan, B.; et al. Nanoparticle-Stabilized Capsules for the Treatment of Bacterial Biofilms. *ACS Nano* **2015**, *9*, 7775−7782.
(21) Herzig, E. M.; White, K. A.; Schofield, A. B.; Poon, W. C. K.; Clegg, P. S. Bicontinuous emulsions stabilized solely by colloidal particles. *Nat. Mater.* **2007**, *6*, 966.
(22) Stratford, K.; Adhikari, R.; Pagonabarraga, I.; Desplat, J. C.; Cates, M. E. Colloidal jamming at interfaces: A route to fluid-bicontinuous gels. *Science* **2005**, *309*, 2198−2201.
(23) Miguel, A. S.; Scrimgeour, J.; Curtis, J. E.; Behrens, S. H. Smart colloidosomes with a dissolution trigger. *Soft Matter* **2010**, *6*, 3163.
(24) Montelongo, Y.; et al. Electrotunable nanoplasmonic liquid mirror. *Nat. Mater.* **2017**, *16*, 1127−1135.
(25) Guzman, E.; et al. Particle-laden fluid/fluid interfaces: physico-chemical foundations. *J. Phys.: Condens. Matter* **2021**, *33*, 37.
(26) Paunov, V. N.; Binks, B. P.; Ashby, N. P. Adsorption of charged colloid particles to charged liquid surfaces. *Langmuir* **2002**, *18*, 6946−6955.
(27) Dunstan, D. E.; Saville, D. A. Electrokinetic Potential of the Alkane Aqueous-Electrolyte Interface. *J. Chem. Soc., Faraday Trans.* **1993**, *89*, 527−529.
(28) Marinova, K. G.; et al. Charging of oil-water interfaces due to spontaneous adsorption of hydroxyl ions. *Langmuir* **1996**, *12*, 2045.
(29) Creux, P.; Lachaise, J.; Graciaa, A.; Beattie, J. K.; Djerdjev, A. M. Strong Specific Hydroxide Ion Binding at the Pristine Oil/Water and Air/Water Interfaces. *J. Phys. Chem. B* **2009**, *113*, 14146−14150.
(30) Stachurski, J.; Michalek, M. The effect of the zeta potential on the stability of a non-polar oil-in-water emulsion. *J. Colloid Interface Sci.* **1996**, *184*, 433−436.
(31) Dickinson, W. The effect of pH upon the electrophoretic mobility of emulsions of certain hydrocarbons and aliphatic halides. *Trans. Faraday Soc.* **1941**, *37*, 140−147.
(32) Beattie, J. K.; Djerdjev, A. M. The pristine oil/water interface: Surfactant-free hydroxide-charged emulsions. *Angew. Chem., Int. Ed.* **2004**, *43*, 3568−3571.
(33) Zangi, R.; Engberts, J. B. F. N. Physisorption of hydroxide ions from aqueous solution to a hydrophobic surface. *J. Am. Chem. Soc.* **2005**, *127*, 2272−2276.
(34) Kudin, K. N.; Car, R. Why are water-hydrophobic interfaces charged? *J. Am. Chem. Soc.* **2008**, *130*, 3915−3919.
(35) Levin, Y.; dos Santos, A. P.; Diehl, A. Ions at the Air-Water Interface: An End to a Hundred-Year-Old Mystery? *Phys. Rev. Lett.* **2009**, *103*, No. 257802.
(36) Mundy, C. J.; Kuo, I. F. W.; Tuckerman, M. E.; Lee, H. S.; Tobias, D. J. Hydroxide anion at the air-water interface. *Chem. Phys. Lett.* **2009**, *481*, 2−8.
(37) Gray-Weale, A.; Beattie, J. K. An explanation for the charge on water's surface. *Phys. Chem. Chem. Phys.* **2009**, *11*, 10994−11005.
(38) Wang, Z. Y.; Zhang, P. L.; Ma, Z. W. On the physics of both surface overcharging and charge reversal at heterophase interfaces. *Phys. Chem. Chem. Phys.* **2018**, *20*, 4118−4128.
(39) Mbamala, E. C.; von Grunberg, H. H. Effective interaction of a charged colloidal particle with an air-water interface. *J. Phys.: Condens. Matter* **2002**, *14*, 4881−4900.
(40) Danov, K. D.; Kralchevsky, P. A.; Ananthapadmanabhan, K. P.; Lips, A. Particle-interface interaction across a nonpolar medium in relation to the production of particle-stabilized emulsions. *Langmuir* **2006**, *22*, 106−115.
(41) Oettel, M. Entrapment of charged, nonwetting colloids near oil-water interfaces. *Phys. Rev. E: Stat., Nonlinear, Soft Matter Phys.* **2007**, *76*, No. 041403.
(42) Wang, H. Z.; Singh, V.; Behrens, S. H. Image Charge Effects on the Formation of Pickering Emulsions. *J. Phys. Chem. Lett.* **2012**, *3*, 2986.
(43) Dugyala, V. R.; Muthukuru, J. S.; Mani, E.; Basavaraj, M. G. Role of electrostatic interactions in the adsorption kinetics of nanoparticles at fluid-fluid interfaces. *Phys. Chem. Chem. Phys.* **2016**, *18*, 5499−5508.
(44) Simovic, S.; Prestidge, C. A. Nanoparticles of varying hydrophobicity at the emulsion droplet-water interface: Adsorption and coalescence stability. *Langmuir* **2004**, *20*, 8357−8365.
(45) Marina, P. F.; Xu, J.; Wu, X.; Xu, H. L. Thinking outside the box: placing hydrophilic particles in an oil phase for the formation and stabilization of Pickering emulsions. *Chem. Sci.* **2018**, *9*, 4821−4829.
(46) Zhang, Y.; et al. Interfacial Activity of Nonamphiphilic Particles in Fluid-Fluid Interfaces. *Langmuir* **2017**, *33*, 4511−4519.
(47) Larson-Smith, K.; Jackson, A.; Pozzo, D. C. SANS and SAXS Analysis of Charged Nanoparticle Adsorption at Oil-Water Interfaces. *Langmuir* **2012**, *28*, 2493−2501.
(48) Reincke, F.; et al. Understanding the self-assembly of charged nanoparticles at the water/oil interface. *Phys. Chem. Chem. Phys.* **2006**, *8*, 3828−3835.
(49) Zheng, R. J.; Binks, B. P.; Cui, Z. G. Pickering Emulsions of Hydrophilic Silica Particles and Symmetrical Organic Electrolytes. *Langmuir* **2020**, *36*, 4619−4629.
(50) Midmore, B. R. Preparation of a novel silica-stabilized oil/water emulsion. *Colloids Surf., A* **1998**, *132*, 257−265.
(51) Ridel, L.; Bolzinger, M. A.; Gilon-Delepine, N.; Dugas, P. Y.; Chevalier, Y. Pickering emulsions stabilized by charged nanoparticles. *Soft Matter* **2016**, *12*, 7564−7576.
(52) Hassander, H.; Johansson, B.; Tornell, B. The Mechanism of Emulsion Stabilization by Small Silica (Ludox) Particles. *Colloids Surf.* **1989**, *40*, 93−105.
(53) Su, B.; et al. Reversible voltage-induced assembly of Au nanoparticles at liquid vertical bar liquid interfaces. *J. Am. Chem. Soc.* **2004**, *126*, 915.
(54) Collins, M. C.; Hebrant, M.; Herzog, G. Ion transfer at polarised liquid-liquid interfaces modified with adsorbed silica nanoparticles. *Electrochim. Acta* **2018**, *282*, 155−162.
(55) Hung, L. Q. Electrochemical Properties of the Interface between 2 Immiscible Electrolyte Solutions. Part 1. Equilibrium Situation and Galvani Potential Difference. *J. Electroanal. Chem.* **1980**, *115*, 159−174.
(56) Leunissen, M. E.; van Blaaderen, A.; Hollingsworth, A. D.; Sullivan, M. T.; Chaikin, P. M. Electrostatics at the oil-water interface, stability, and order in emulsions and colloids. *Proc. Natl. Acad. Sci. U. S. A.* **2007**, *104*, 2585−2590.
(57) Leunissen, M. E.; Zwanikken, J.; van Roij, R.; Chaikin, P. M.; van Blaaderen, A. Ion partitioning at the oil-water interface as a source of tunable electrostatic effects in emulsions with colloids. *Phys. Chem. Chem. Phys.* **2007**, *9*, 6405−6414.
(58) Elbers, N. A.; et al. Repulsive van der Waals forces enable Pickering emulsions with non-touching colloids. *Soft Matter* **2016**, *12*, 7265−7272.
(59) Everts, J. C.; Samin, S.; van Roij, R. Tuning Colloid-Interface Interactions by Salt Partitioning. *Phys. Rev. Lett.* **2016**, *117*, No. 098002.
(60) Reid, J. D.; Melroy, O. R.; Buck, R. P. Double-Layer Charge and Potential Profiles at Immiscible Liquid Electrolyte Interfaces. *J. Electroanal. Chem.* **1983**, *147*, 71−82.
(61) Luo, G. M.; et al. Ion distributions near a liquid-liquid interface. *Science* **2006**, *311*, 216−218.
(62) Luo, G. M.; et al. Ion distributions at the nitrobenzene-water interface electrified by a common ion. *J. Electroanal. Chem.* **2006**, *593*, 142−158.

https://doi.org/10.1021/acs.langmuir.1c02919
Langmuir 2022, 38, 2821−2831

(63) Royall, C. P.; Leunissen, M. E.; van Blaaderen, A. A new colloidal model system to study long-range interactions quantitatively in real space. *J. Phys.: Condens. Matter* **2003**, *15*, S3581−S3596.
(64) Stewart, H. L.; et al. Nanoparticle metrology of silica colloids and super-resolution studies using the ADOTA fluorophore. *Meas. Sci. Technol.* **2016**, *27*, No. 045007.
(65) Uricanu, V.; Eastman, J. R.; Vincent, B. Stability in colloidal mixtures containing particles with a large disparity in size. *J. Colloid Interface Sci.* **2001**, *233*, 1−11.
(66) Koroleva, M. Y.; Bydanov, D. A.; Palamarchuk, K. V.; Yurtov, E. V. Stabilization of Oil-in-Water Emulsions with SiO_2 and Fe_3O_4 Nanoparticles. *Colloid J.* **2018**, *80*, 282−289.
(67) Dunstan, D. E. Temperature-Dependence of the Electrokinetic Properties of 2 Disparate Surfaces. *J. Colloid Interface Sci.* **1994**, *166*, 472−475.
(68) Dunstan, D. E.; Saville, D. A. Electrophoretic Mobility of Colloidal Alkane Particles in Electrolyte-Solutions. *J. Chem. Soc., Faraday Trans.* **1992**, *88*, 2031−2033.
(69) Vazdar, M.; Pluharova, E.; Mason, P. E.; Vacha, R.; Jungwirth, P. Ions at Hydrophobic Aqueous Interfaces: Molecular Dynamics with Effective Polarization. *J. Phys. Chem. Lett.* **2012**, *3*, 2087−2091.
(70) Vacha, R.; et al. The Orientation and Charge of Water at the Hydrophobic Oil Droplet-Water Interface. *J. Am. Chem. Soc.* **2011**, *133*, 10204.
(71) Cui, M. M.; Emrick, T.; Russell, T. P. Stabilizing Liquid Drops in Nonequilibrium Shapes by the Interfacial Jamming of Nanoparticles. *Science* **2013**, *342*, 460−463.
(72) Bera, M. K.; et al. Interfacial Localization and Voltage-Tunable Arrays of Charged Nanoparticles. *Nano Lett.* **2014**, *14*, 6816−6822.
(73) Binks, B. P.; Yin, D. Z. Pickering emulsions stabilized by hydrophilic nanoparticles: in situ surface modification by oil. *Soft Matter* **2016**, *12*, 6858−6867.
(74) Rutland, M. W.; Pashley, R. M. The Charging Properties of Monodisperse Colloidal Silica in Symmetrical Quaternary Ammonium Ion Solutions. *J. Colloid Interface Sci.* **1989**, *130*, 448−456.
(75) Van der Donck, J. C. J.; Vaessen, G. E. J.; Stein, H. N. Adsorption of Short-Chain Tetraalkylammonium Bromide on Silica. *Langmuir* **1993**, *9*, 3553−3557.
(76) Tamaki, K. The Surface Activity of Tetra-*n*-alkylammonium Halides in Aqueous Solutions. The Effect of Hydrophobic Hydration. *Bull. Chem. Soc. Jpn.* **1974**, *47*, 2764−2767.
(77) Verwey, E. J. W.; Niessen, K. F.; Philips, N. V. The electrical double layer at the interface of two liquids. *Philos. Mag.* **1939**, *28*, 435.
(78) Zwanikken, J.; de Graaf, J.; Bier, M.; van Roij, R. Stability of additive-free water-in-oil emulsions. *J. Phys.: Condens. Matter* **2008**, *20*, No. 494238.
(79) Zwanikken, J.; van Roij, R. Charged colloidal particles and small mobile ions near the oil-water interface: Destruction of colloidal double layer and ionic charge separation. *Phys. Rev. Lett.* **2007**, *99*, No. 178301.
(80) Evans, D. F.; Wennerström, H. *The Colloidal Domain: Where Physics, Chemistry, Biology, and Technology Meet*; John Wiley & Sons, 1999.
(81) Electrochemical Database (École Polytechnique Fédérale de Lausanne (EPFL), http://sbsrv7.epfl.ch/instituts/isic/lepa/).
(82) Laanait, N.; et al. Tuning ion correlations at an electrified soft interface. *Proc. Natl. Acad. Sci. U. S. A.* **2012**, *109*, 20326−20331.
(83) Marcus, Y. Ionic Radii in Aqueous Solutions. *Chem. Rev.* **1988**, *88*, 1475−1498.

Recommended by ACS

Adsorption Dynamics of Surface-Modified Silica Nanoparticles at Solid–Liquid Interfaces
Mohammad Ali Khazaei, Azadeh Kordzadeh, *et al.*
SEPTEMBER 30, 2022
LANGMUIR
READ

How Particle Deformability Influences the Surfactant Distribution in Colloidal Polymer Films
Toby R. Palmer, Joseph L. Keddie, *et al.*
OCTOBER 04, 2022
LANGMUIR
READ

Impact of Particle Sedimentation in Pendant Drop Tensiometry
Roy J. B. M. Delahaije, Jack Yang, *et al.*
AUGUST 09, 2022
LANGMUIR
READ

Plant Latex as a Versatile and Sustainable Emulsifier
Hemant Kumar and Madivala G. Basavaraj
OCTOBER 21, 2022
LANGMUIR
READ

Get More Suggestions >

https://doi.org/10.1021/acs.langmuir.1c02919
Langmuir 2022, 38, 2821−2831